

Gamut Mapping Based on Color Space Division for Enhancement of Lightness Contrast and Chrominance

Yang-Ho Cho, Yun-Tae Kim and Yeong-Ho Ha[▲]

School of Electrical Engineering and Computer Science, Kyungpook National University, Taegu, Korea

Cheol-Hee Lee[▲]

Major of Computer Engineering, Andong National University, Gyeongbuk, Korea

This article proposes a gamut mapping algorithm based on color space division for cross media color reproduction. Since all color devices have a limited range of producible colors, the colors reproduced by a destination device will invariably differ from those of the original device. Accordingly, to reduce the color difference between devices, the proposed method divides the whole gamut into parabolic shapes based on the intersection between the lightness tolerance scale and the boundary of the original gamut. This division of the gamut into parabolic shapes and piecewise mapping of each region facilitates both consideration of the gamut characteristics and mapping uniformity. In addition, since the human visual system is more sensitive to lightness variations, the use of a lightness tolerance scale only permits unperceivable lightness mapping variations. As a result, the proposed algorithm is able to reproduce high quality color images even with low cost color devices.

Journal of Imaging Science and Technology 48: 66–74 (2004)

Introduction

The color consistency between display devices is important when color is a key feature in identifying an object. Currently, when a color image is represented on a monitor and then reproduced on a printer, the images are very different. This phenomenon can be explained by various reasons that may work independently or in combination, for example, the type of surrounding light, difference in the color calibration, and color gamut difference between the devices. Among these factors, the color gamut, which is the reproducible color range for a device, has the predominant effect on such a color difference.¹ Therefore, effective color gamut mapping is essential to obtain color consistency.

Gamut mapping methods are classified into gamut mapping direction and gamut mapping methods.^{2,3} Mapping direction methods are defined as those where the out-of-gamut colors are mapped into the gamut. Gamut

mapping methods deal with how the colors are mapped in a given direction. Gamut mapping direction methods are classified into three types according to which human visual color attribute is used to map the colors. Gamut mapping algorithms are usually performed in a uniform color space to facilitate the separation of lightness, chrominance, and hue. Among these color attributes, if only lightness or chrominance is used, this is called one-dimensional gamut mapping. As such, since one-dimensional gamut mapping only uses one color attribute, this results in unavoidable problems. The gamut mapping methods proposed by Morovic or Hezog use lightness and chrominance simultaneously on a constant hue plane.^{2,4} Such methods are referred to as two-dimensional gamut mapping, and since the human visual system is more sensitive to hue variations, lightness and chrominance are used. Recently, three-dimensional gamut mapping was proposed by Katoh and Chen, based on considering lightness, chrominance, and hue at the same time.^{2,5}

Gamut mapping methods include color gamut clipping, linear compression and nonlinear compression, etc.^{6,7} The clipping method maps all the colors outside the gamut onto the surface of the reproduction gamut. Linear compression linearly compresses all the colors in the original gamut into the reproduction gamut. Nonlinear compression maps all the colors in the original gamut onto the reproduction gamut according to nonlinear functions. If the gamut difference is minimal, the best mapping method is the clipping method.

In this study, to preserve color consistency between the original and reproduction device, the proposed

Original manuscript received February 13, 2003

▲ IS&T Member

Color Plates 5 through 9 can be found in the color plate section of this issue; pp. 75–83.

©2004, IS&T—The Society for Imaging Science and Technology

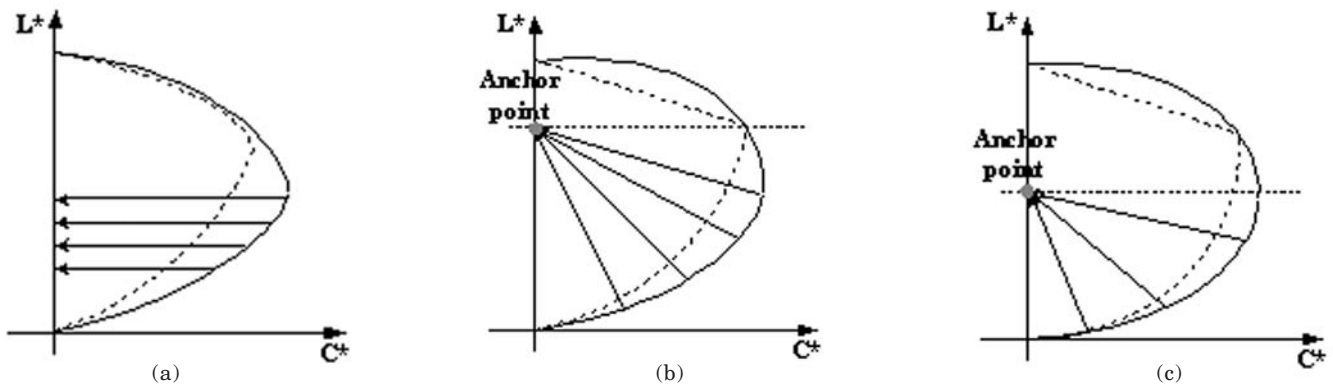


Figure 1. Conventional gamut mapping algorithms; (a) one-dimensional linear chrominance mapping along lines of constant lightness. (b) two-dimensional mapping toward the lightness value of the maximum chrominance on each hue plane. (c) two-dimensional mapping toward middle lightness value on L^* axis.

method divides the whole gamut into parabolic shapes in CIEL*a*b* color space, then applies a piecewise mapping process for each divided region. As a result, the proposed mapping method is able to enhance the lightness contrast and chrominance, as it is based on the shape and characteristics of each gamut. In addition, since the human visual system is more sensitive to changes in hue, the proposed method applies the two-dimensional clipping method where lightness and chrominance are simultaneously used to map out-of-gamut colors to the gamut boundary of the reproduction device on a constant hue plane.

Conventional Gamut Mapping Methods

By reducing the color difference, conventional anchor point gamut mapping algorithms attempt to map all out-of-gamut colors in the L^* - C^* plane (at a constant hue) toward single or multiple convergence points.^{1,2,8,9} However these methods do not consider the gamut characteristics and mapping uniformity. Consequently, the output image includes significant changes in the lightness and chrominance at the extremities of the lightness axis and in high chrominance regions. Figure 1(a) shows linear chrominance mapping along the lines of constant lightness. Figure 1(b) maps lightness and chrominance toward the lightness value of the maximum chrominance on each hue plane, referred to as the anchor point on the L^* axis of the reproduction gamut. This method cannot preserve the original lightness contrast and chrominance. After mapping, the lightness dynamic range is reduced because the lightness in the high lightness regions is decreased, while the lightness in the low lightness regions is increased, plus a large chrominance change occurs in the high chrominance regions. Figure 1(c) uses a similar method to Fig. 1(b), where the anchor point is the central point on the L^* axis of the reproduction gamut.

To overcome problems related to single anchor point methods, variable anchor point methods have been proposed.^{8,9} Figure 2 shows the variable anchor point methods proposed by Lee. These methods set variable anchor points in each region based on the relationship of CUSP points between the monitor and printer gamuts. Recently more flexible methods have been proposed according to the topography of the gamut.¹⁰ However, there is still a non-mapping uniformity in each region and no consideration is given to the relationship between the lightness and chrominance and the overall gamut characteristics.

Color Space Conversion

Generally, gamut mapping is performed in a perceptually uniform color space. As such, the proposed gamut mapping algorithm is performed in CIEL*a*b* color space, and, since color devices all have a device-dependent color space, this has to be converted into a uniform color space for general application. The gamuts are first determined based on measuring color samples including colors that cover the majority of the color space for each device. From these measurements, a color space conversion is then performed using a tetrahedral interpolation,¹⁰ which can be performed with fewer multiplications and is an easier coefficient calculation for weighted averages. Figure 3 shows the tetrahedral division of a subcube in RGB color space and under tetrahedral conditions. All the cubes are divided into six tetrahedra to generate look-up tables for the gamut. Each element in the look-up tables represents a tetrahedron and has measured L^* a*b* values for the four vertices of each tetrahedron. After composing look-up tables for all the tetrahedra, these equations are then used to determine whether the input color is included within the tetrahedra and calculate the weighting factor for the interpolation.

$$\begin{bmatrix} \alpha \\ \beta \\ \gamma \end{bmatrix} \begin{bmatrix} r_1 - r_0 & r_2 - r_0 & r_3 - r_0 \\ g_1 - g_0 & g_2 - g_0 & g_3 - g_0 \\ b_1 - b_0 & b_2 - b_0 & b_3 - b_0 \end{bmatrix}^{-1} \begin{bmatrix} r_p - r_0 \\ g_p - g_0 \\ b_p - b_0 \end{bmatrix}, \quad (1)$$

where α, β, γ are the weighting factors, r_p, g_p, b_p are the input colors, and $r_{1,2,3}, g_{1,2,3}, b_{1,2,3}$ represent the stored RGB values for each tetrahedron in the look-up tables. The condition that the input color is included in the tetrahedra is as follows:

$$\alpha \geq 0, \beta \geq 0, \gamma \geq 0 \text{ and } \alpha + \beta + \gamma \leq 1, \quad (2)$$

The weighting factor that satisfies this condition is then used to interpolate the input RGB color, and the interpolated color in CIEL*a*b* is

$$\begin{bmatrix} L_p \\ a_p \\ b_p \end{bmatrix} = \begin{bmatrix} L_1 - L_0 & L_2 - L_0 & L_3 - L_0 \\ a_1 - a_0 & a_2 - a_0 & a_3 - a_0 \\ b_1 - b_0 & b_2 - b_0 & b_3 - b_0 \end{bmatrix} \begin{bmatrix} \alpha \\ \beta \\ \gamma \end{bmatrix} + \begin{bmatrix} L_0 \\ a_0 \\ b_0 \end{bmatrix}, \quad (3)$$

where L_p, a_p, b_p is the interpolated color and $L_{1,2,3}, a_{1,2,3}, b_{1,2,3}$ represent the stored CIEL*a*b* values for each

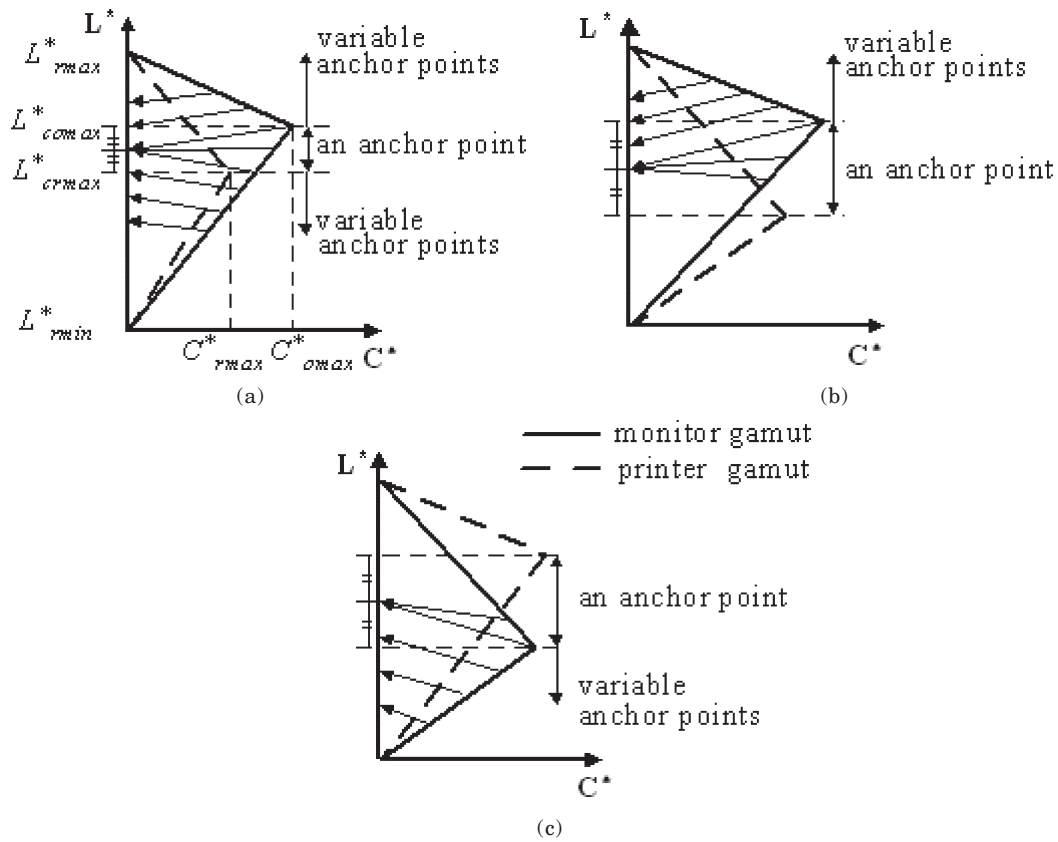


Figure 2. Gamut mapping based on variable anchor points: (a) monitor gamut includes printer gamut; (b) monitor gamut partially includes printer gamut and monitor CUSP point is larger than printer CUSP point; (c) monitor gamut partially includes printer gamut and monitor CUSP point is smaller than printer CUSP point.

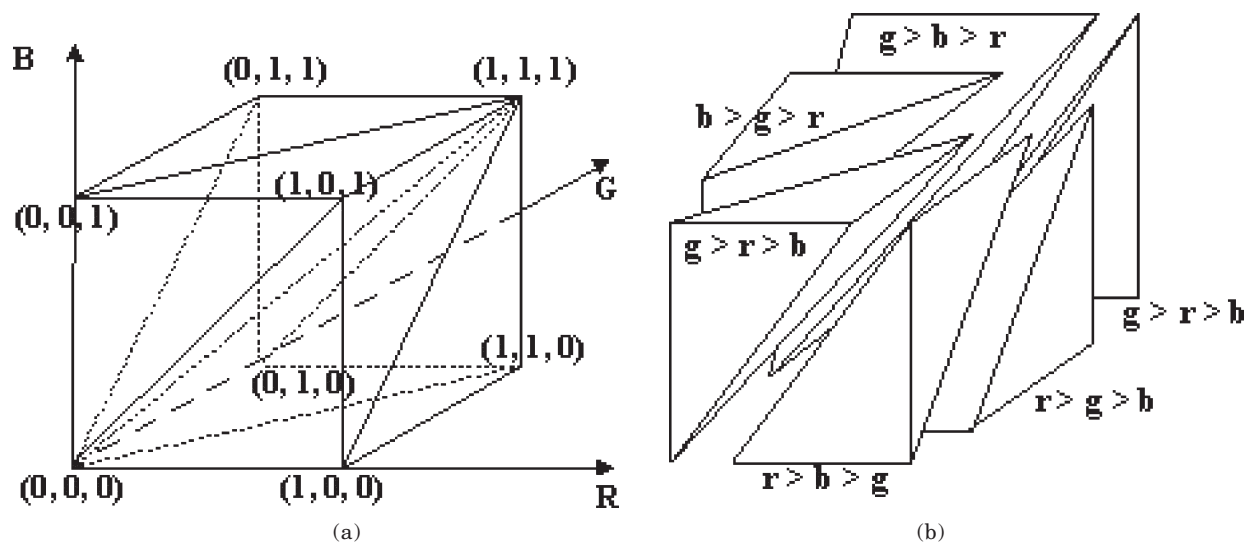


Figure 3. Tetrahedral division of subcube; (a) location of the tetrahedral points in subcube; (b) equations of each tetrahedral conditions.

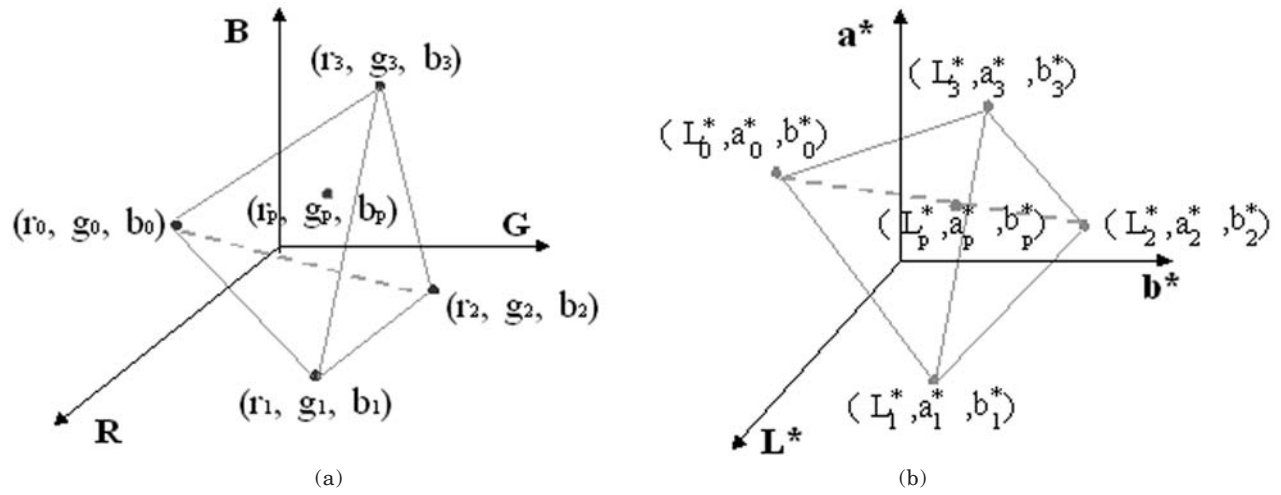


Figure 4. Corresponding tetrahedrons in two spaces. (a) RGB color space and (b) CIEL*a*b* color space.

tetrahedron in the look-up tables. Figure 4 shows the corresponding tetrahedrons in the two color spaces, i.e., RGB and CIEL*a*b*. In this study, the interpolation from RGB color space to CIEL*a*b* color space is defined as a forward interpolation, while the interpolation from CIEL*a*b* color space to CMY color space is defined as a backward interpolation.

Intersecting Points at Gamut Boundary

To map all the out-of-gamut colors to the gamut boundary, it is necessary to find the intersecting point between gamut boundary and line. Figure 5 shows this relationship used to find the intersecting point. Out-of-gamut color is L_4, a_4, b_4 , and the point on the achromatic color axis is L_0, a_0, b_0 . The triangle in Fig. 5 is assumed to be included within the gamut boundary. The vertical unit vector in a triangle, $[a, b, c]$, is calculated as follows:

$$[a, b, c] = [1 \ 1 \ 1] \cdot \begin{bmatrix} L_1 & L_2 & L_3 \\ a_1 & a_2 & a_3 \\ b_1 & b_2 & b_3 \end{bmatrix}^{-1}, \quad (4)$$

To determine whether the line cuts across the triangle, we find the inner product between the unit vector and the line,

$$\delta = [1 \ 1 \ 1] \cdot \begin{bmatrix} L_1 & L_2 & L_3 \\ a_1 & a_2 & a_3 \\ b_1 & b_2 & b_3 \end{bmatrix}^{-1} \cdot \begin{bmatrix} L_0 - L_4 \\ a_0 - a_4 \\ b_0 - b_4 \end{bmatrix}, \quad (5)$$

if the value of δ is not equal to 0, it means the line cuts across the triangle. And then the distance, η , between the intersecting point and L_4, a_4, b_4 is calculated as follows:

$$\eta = \frac{1 - [a \ b \ c] \cdot \begin{bmatrix} L_4 \\ a_4 \\ b_4 \end{bmatrix}}{\delta}. \quad (6)$$

At last, the intersecting point L_p, a_p, b_p is

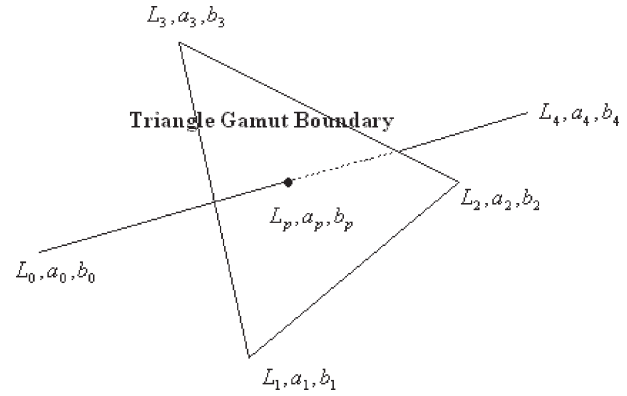


Figure 5. Intersecting point between out-of-gamut pixel and gamut boundary.

$$\begin{bmatrix} L_p \\ a_p \\ b_p \end{bmatrix} = \eta \cdot \begin{bmatrix} L_0 - L_4 \\ a_0 - a_4 \\ b_0 - b_4 \end{bmatrix} + \begin{bmatrix} L_4 \\ a_4 \\ b_4 \end{bmatrix}. \quad (7)$$

Color Space Division

This article proposes a gamut mapping method based on color space division and region-by-region mapping to promote image contrast and mapping uniformity. Figure 6 shows a flowchart of the proposed algorithm. The target color devices are a monitor and printer. First, the device dependent color space is converted into a device independent color space using a forward tetrahedral interpolation. In CIEL*a*b* color space, the lightness of the blacks between two gamuts is often different. Therefore, lightness mapping is also performed to include the lightness range of the input image within the printer gamut. This process can be expressed as

$$L_o = \frac{(L_i - L_{m \min}) \times (L_{p \max} - L_{p \min})}{L_{m \max} - L_{m \min}} + L_{p \min}$$

$$\begin{aligned} a_o &= a_i \\ b_o &= b_i \end{aligned}, \quad (8)$$

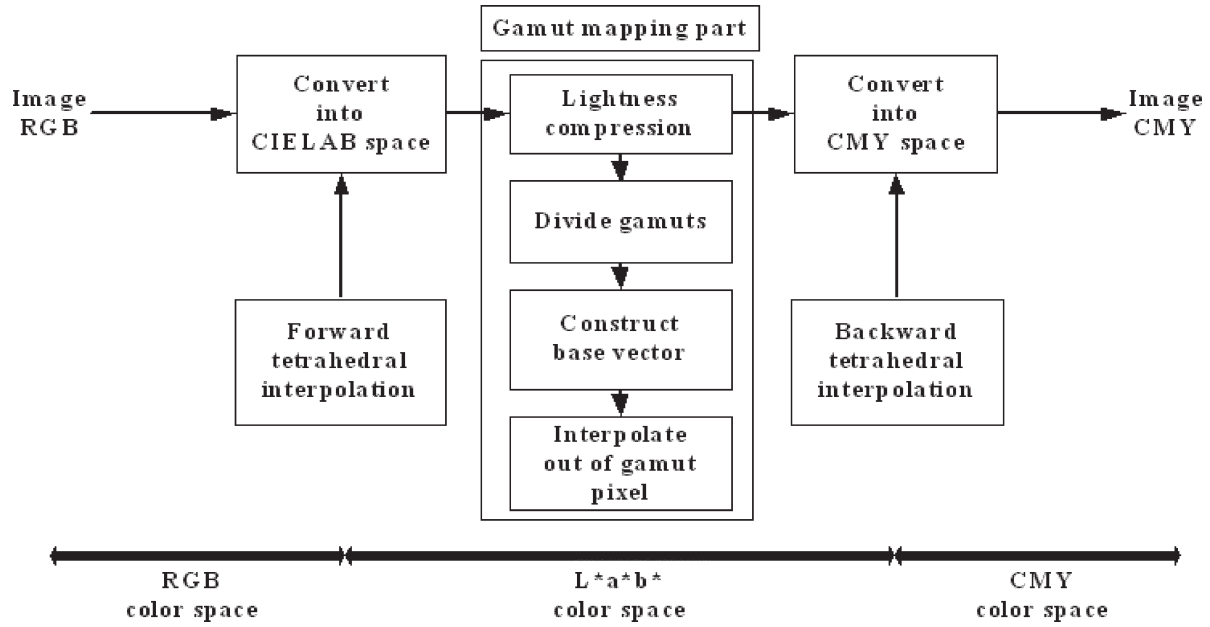


Figure 6. Block diagram of proposed gamut mapping method based on color space division.

where L_o, a_o, b_o is the output of the lightness mapping, L_{max}, L_{min} is maximum and minimum lightness of monitor gamut and L_{pmax}, L_{pmin} is maximum and minimum lightness of printer gamut. A linear lightness compression method is used, then each gamut is divided into parabolic shapes to cover the entire gamut. Using the divided regions, base vectors are calculated at each region and piecewise gamut mapping is executed by interpolating all the out-of-gamut colors. As such, the proposed algorithm can consider the gamut characteristics and determine an effective mapping direction.

Lightness Tolerance Scale

The method used for dividing regions is based on a lightness tolerance scale. The human visual system is more sensitive to variations in lightness variations; accordingly, it is more effective to restrict lightness changes after gamut mapping. In CIEL*a*b* color space, the lightness tolerance scale is generally around 3,¹² which is used to divide the gamut and restrict the lightness changes to an imperceptible level. In particular, lower lightness scales are selected to divide a gamut, as they are more effective in enhancing a low contrast and including the whole gamut. Selecting lower lightness tolerance values below the middle lightness for each hue plane does not affect the high lightness values. Consequently, lightness tolerance scales can be used as the standard for dividing a gamut into regions.

Parabolic Function for Dividing Gamut

The proposed gamut mapping method is based on region-by-region mapping. It is assumed that the hue angle remains constant; then the lightness-chrominance color space of each gamut is divided using the lightness tolerance scales and original gamut boundary. First, the intersecting points between the lightness tolerance scales and the original gamut boundary are determined, then the gamut is divided using a parabolic function, as shown in Fig. 7. The relationship between the lightness and chrominance to be divided is defined as follows:

$$(L^* - L_{middle})^2 = 4 \times C^* \times C_{max} \\ C_{max} = \max(C_m), \quad L_{middle} = (L_{max} + L_{min}) / 2 \quad (9)$$

where C_m is the chrominance of monitor gamut and L_{middle} is the middle point of lightness for each hue plane. The focal point of the parabolic function is the maximum chrominance on each hue plane to include the whole gamut, as such, C_{max} is calculated for each hue plane. The parabolic function used to divide the gamut can be changed according to each gamut shape. Thus it not only considers the gamut characteristics, but also includes the whole gamut, as the parabolic function takes the inverse shape of each gamut. In addition, the shape of the parabolic function is changed according to the distance of the focal point. The more distant the focal point from (C_{max}, L_{middle}) to the right, the narrower the parabolic function, while the more distant from (C_{max}, L_{middle}) to the left, the wider the parabolic function. That is, since the shape of parabolic function varies with the focal point, it can cover all the other functions. Therefore, for general application, a parabolic function is selected to divide the gamut and determine the mapping direction.

Direction of Gamut Mapping and Interpolation Method

In Fig. 7, the gamut is divided by a parabolic function based on the intersecting points between the lightness tolerance scales and the original gamut boundary. The divided regions are then the basic units used to determine the mapping direction. Thereafter, the region-by-region clipping method is applied, according to the determined mapping direction. Figure 8 shows the specific mapping directions and interpolation method. First, the intersecting points are set between the lower lightness values and the monitor gamut boundary ($i_1, i_2, i_3, i_4 \dots$). In this article, the number of intersecting points is 8 for each hue plane to avoid a complex algorithm. Second, base vectors are constructed using the inter-

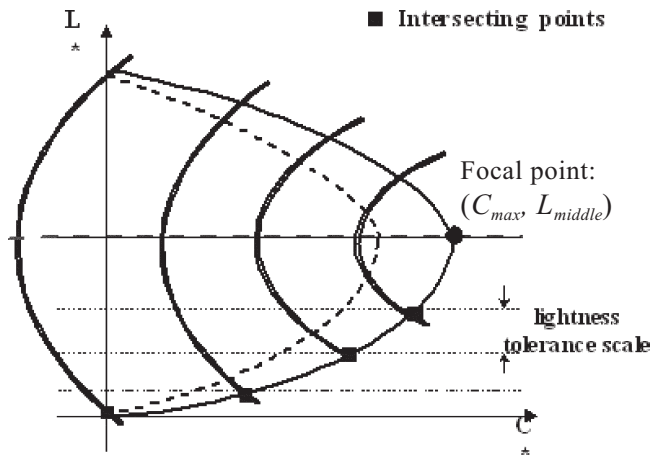


Figure 7. Dividing the gamut with parabolic function based on intersecting points between lightness tolerance scale and monitor gamut boundary.

secting points between the parabolic function and the monitor and printer gamut boundaries for each divided region. Each parabolic function is

$$(L_n^* - L_{middle})^2 = 4 \times C_n^* \times C_{max}, \quad n = 1, 2, 3, \dots, 8. \quad (10)$$

The shape of the parabolic function changes according to the C_{max} and n for each hue plane. Since the mapping direction is determined by the parabolic function, if the parabolic function is close to the focal point, the slope of the mapping direction will be high, indicating that the chrominance will be preserved rather than the lightness in a high chrominance region after mapping. Conversely, if the parabolic function is far from the focal point, the slope of the mapping direction will be low, indicating that the lightness will be preserved rather than the chrominance at the extremities of the lightness axis. This piecewise mapping then maintains the

saturation of the original image in the reproduction, because the slope of the mapping direction is constant in each region. These mapping characteristics also enhance the vividness of the original image. Third, all out-of-gamut pixels are mapped to the printer gamut boundary through interpolation using base vectors. For example, if the intersecting points between the gamut boundaries and the parabolic function are m_1 , m_2 , p_1 , and p_2 respectively in Fig. 8, m_1p_1 and m_2p_2 can be constructed as the base vectors to determine the mapping direction. Once the mapping direction is determined, the distance between the out-of-gamut color and the base vectors can be calculated. Next, the cross points between extending the base vectors and the achromatic axis are determined, then the point on the achromatic color axis of the out-of-gamut color is calculated considering the calculated distance, using linear interpolation. Finally, an out-of-gamut pixel T_{out} can be mapped as T_{in} based on the interpolation method using the base vectors.

Conventional gamut mapping methods are non-uniform in each region. The CUSP method maps all out-of-gamut colors toward a single convergence point, while the variable anchor point gamut mapping method divides a gamut into three regions. As a result, no consideration is paid to the gamut characteristics or conserving uniform mapping. In contrast, dividing regions using parabolic shapes preserves the chrominance rather than the lightness in a high chrominance region and the lightness rather than the chrominance at the extremities of the lightness axis, plus the uniformity of the mapping direction is improved due to a constant mapping direction in each region. If uniform mapping is not performed in gamut mapping, different characteristics occur in the resulting image. However, the proposed method preserves a constant mapping direction as much as possible using color space division and region-by-region piecewise mapping.

Experimental Results

The proposed algorithm was applied to color gamut mapping from a monitor to a printer. To determine the gamut of each device, $9 \times 9 \times 9$ color samples were generated in RGB space for the monitor (LG Flatron 775FT) and

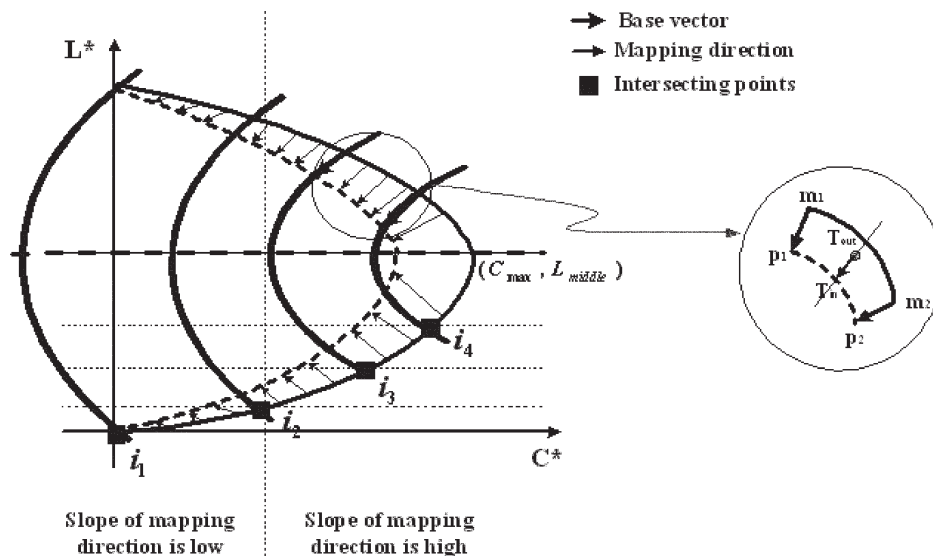


Figure 8. The mapping direction and interpolation method of the proposed gamut mapping.

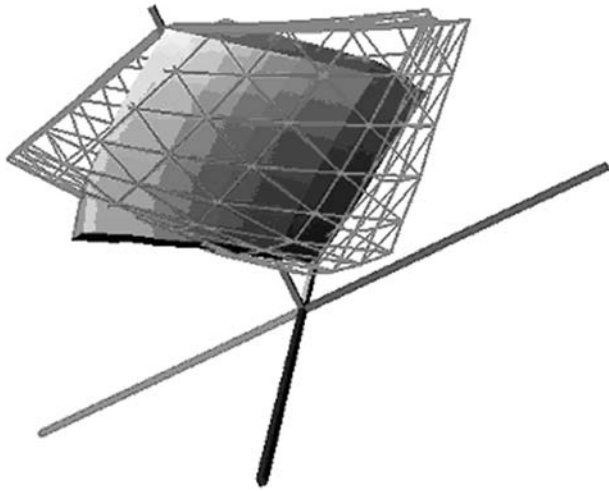


Figure 9. Gamut difference between monitor (mesh) and printer(solid) in CIEL*a*b*.

printed in CMY space for the printer (Hewlett-Packard 895cxi). Figure 9 shows the difference between the monitor and printer gamuts. To measure the sample color

displayed on the monitor and printer, Minolta CS-1000 and Minolta CM-3600d colorimeters were used. The reference illuminant was D65. The representative color samples generated on the monitor and on paper were measured in CIEXYZ color space. From the tristimulus values for the monitor white and paper white, a 3×3 transform matrix was obtained that could map the tristimulus value of the monitor white onto that of the paper white. As a result, all the other color measurement values for the monitor were also rearranged in relation to the paper white. After the white-shift, the measurement values for the samples from the two devices were converted into CIEL*a*b* color space. The device gamuts were obtained from the color samples, and then gamut mapping was performed.

Natural Image Experiments

Five images were chosen to evaluate the general performance of the proposed gamut mapping as shown in Fig. 10. In **Color Plates 5 through 9 (pp. 79–83)**, the images were printed by Floyd–Steinberg error diffusion using various gamut-mapping methods and the proposed method, (a) is the image printed using the linear lightness compression and clipping chrominance method (LL_CC); (b) is the result of the linear lightness compression and linear chrominance compression method (LL_LC); (c) is the result of the CUSP method; (d) is the



Figure 10. Five images are used to compare with each gamut mapping methods.

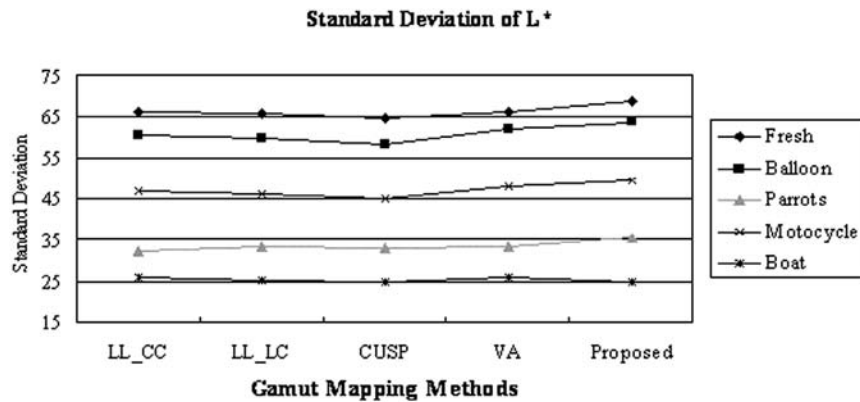


Figure 11. Standard deviation of lightness values compared with the conventional method and proposed method

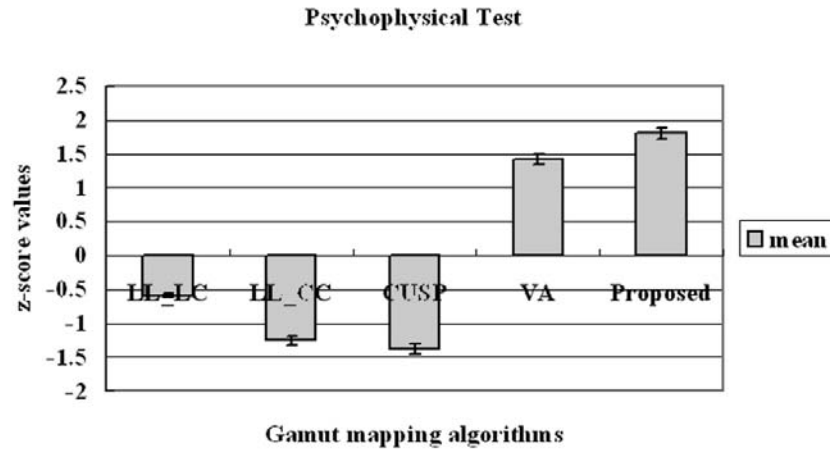


Figure 12. The result of psychophysical test.

result of the variable anchor point method; and (e) is the result of the proposed method. The results of the LL_CC, LL_LC, and CUSP methods, i.e., Color Plates 1 through 5(a), 5(b), and 5(c), all exhibited a low lightness contrast and the maximum chrominance components were all smaller than the result with the proposed method. The results of the LL_CC and LL_LC methods did not reproduce the chrominance effectively due to a constant mapping direction, whereas the results of the CUSP method showed a blocking artifact and the colors were saturated in the mid-tone image, thereby producing a nonlinear tonal distribution. Meanwhile, a better result was acquired using the variable anchor point method, as a variable anchor points was set to map all the out-of-gamut pixels. However, the images reproduced by the proposed method exhibited a higher lightness contrast and more effectively represented the richness of the chrominance in the original image, as such, high chrominance colors were preserved in contrast to the conventional gamut mapping methods in the grape and apple (Color Plate 5, p. 79), balloon (Color Plate 6, p. 80), and feather of parrots (Color Plate 7, p. 81) and the perceived dynamic range was higher in Color Plates 8 and 9 (pp. 82 and 83).

Figure 11 shows the standard deviation of lightness values to compare the conventional methods and the proposed method. Each gamut-mapped image was reproduced in RGB format for easy comparison. As a result, the dynamic range of the proposed method was approximately higher than those of the conventional methods,

indicating that the proposed method enhanced the lightness contrast and chrominance of the images.

Psychophysical Test

A psychophysical experiment was also carried out to compare the gamut mapping between the original monitor image and the printed images. A paired comparison technique was used and both images were evaluated by 15 observers in dim viewing surroundings. The simultaneous binocular viewing technique was used in the paired comparison technique.¹³ Each pair of printed images was shown in a different and random order. The observers were asked to judge how close each sub-image was to the original image on the monitor, then z-score values were used to analyze the results. Figure 12 shows the results of the psychophysical test, where the z-score values were averaged over all images. The horizontal axis shows the gamut mapping methods, while the vertical axis shows the mean interval scale. The results for the proposed method were better than those for the other methods, as the images reproduced by the proposed algorithm were selected as most like those on the monitor.

Conclusion

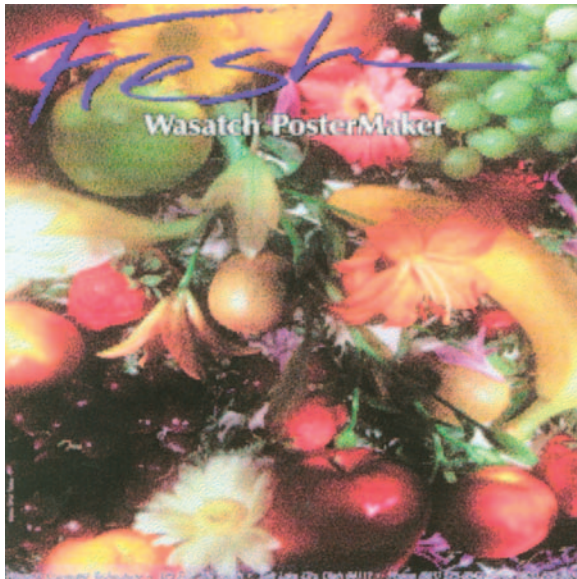
A novel gamut mapping method based on color space division was proposed for printing full resolution color images on limited color output devices. The proposed method divides the whole gamut into parabolic functions based on the intersecting points between the lightness tolerance scales and the original gamut boundary,

thereby restricting the lightness mapping variations. In addition, region-by-region piecewise gamut mapping is used to consider the overall gamut characteristics and determine the optimum mapping direction. As a result, uniform gamut mapping is executed for the entire gamut, which enhances the lightness contrast and chrominance, and the output image is highly consistent with the corresponding input image. ▲

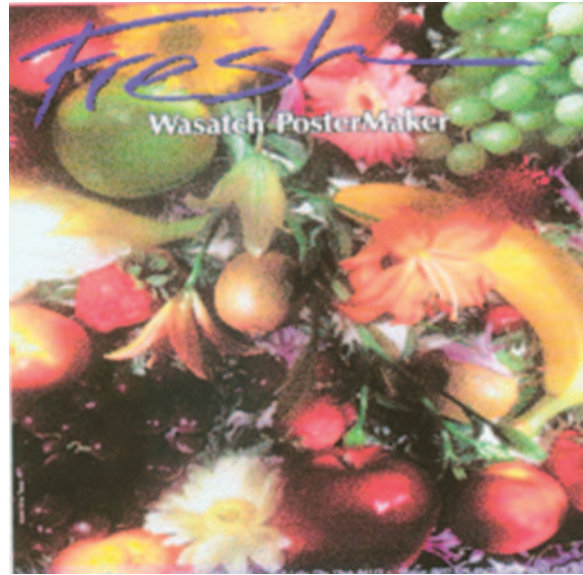
Acknowledgment. This work was supported by grant no. M10203000102-02J0000-04810 from the National Research Laboratory Program of the Korea Ministry of Science & Technology.

References

1. J. Morovic, *To develop a universal colour gamut mapping algorithm*, PhD. Thesis, University of Derby, UK 1998.
2. P. G. Herzog and H. Buring, Optimizing gamut mapping: Lightness and hue adjustment, *J. Imaging Sci. Technol.* **44**(4) 334–342 (2000).
3. N. Katoh, M. Ito and S. Ohno, Three dimensional gamut mapping using various color difference formulae and color spaces, *J. Electron. Imaging* **8**, 365–379 (1999).
4. J. Morovic and M. R. Luo, Evaluation gamut mapping algorithms for universal applicability, *Color Res. Appl.* **26**(1), 85–102 (2001).
5. H. S. Chen and H. Kotera, Three-dimensional gamut mapping method based on the concept of image dependence, *J. Imaging Sci. Technol.* **46**(1), 44–52 (2002).
6. E. D. Montag and M. D. Fairchild, Psychophysical evaluation of gamut mapping techniques using simple rendered images and artificial gamut boundaries, *IEEE Trans. Image Processing*, **6**(7) 977–989 (1997).
7. G. J. Braun and M. D. Fairchild, Image lightness rescaling using sigmoidal contrast enhancement functions, *J. Electron. Imaging* vol. **8**, 380–393, (1999).
8. C. S. Lee, C. H. Lee, and Y. H. Ha, Parametric gamut mapping algorithms using variable anchor points, *J. Imaging Sci. Technol.* **44**, 68–73, (2000).
9. C. S. Lee, Y. W. Park, S. J. Cho, and Y. H. Ha, "Gamut mapping algorithm using lightness mapping and multiple anchor points for linear tone and maximum chroma reproduction, *J. Imaging Sci. Technol.* **45**(3) 209–223 (2001).
10. P. C. Hung, Colorimetric calibration in electronic imaging devices using a look-up-table model and interpolation, *J. Electron. Imaging* **36**(1) 53–61 (1993).
11. L. W. Macdonald, J. Morovic and K. Xiao, A topographic gamut compression algorithm, *J. Imaging Sci. Technol.* **46**(3), 228–236 (2002).
12. E. D. Montag and R. S. Berns, Lightness dependencies and the effect of texture on suprathreshold lightness tolerances, *Color Res. Appl.* **25**(4) (2000).
13. H. S. Chen, M. Omamiyuda and H. Kotera, Gamma-compression gamut mapping method based on the concept of image-to-device, *J. Imaging Sci. Technol.* **45**(2) 141–151 (2001).



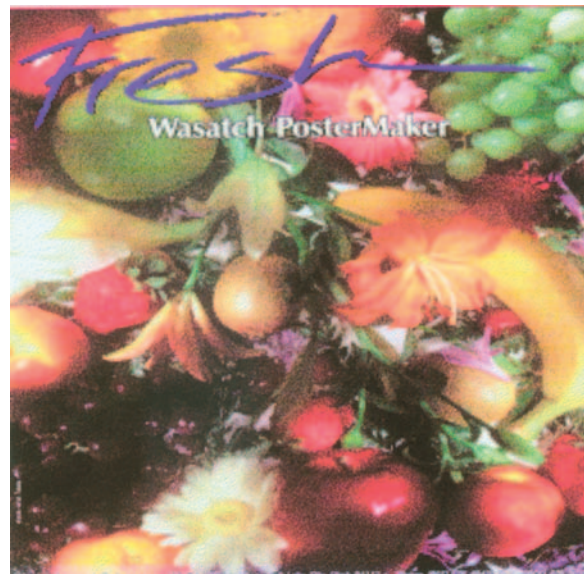
(a)



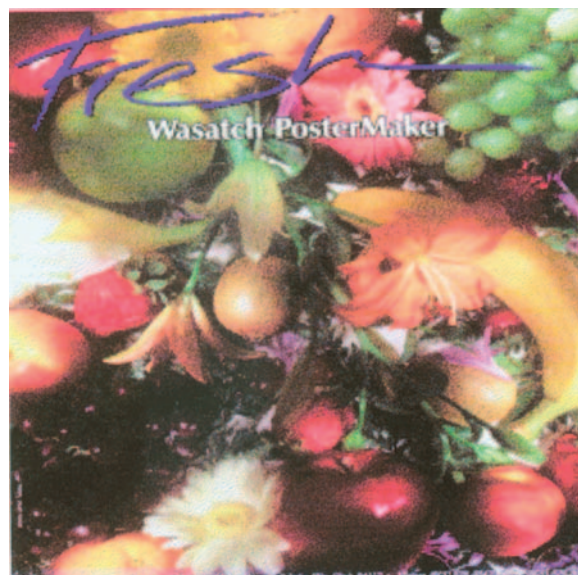
(b)



(c)

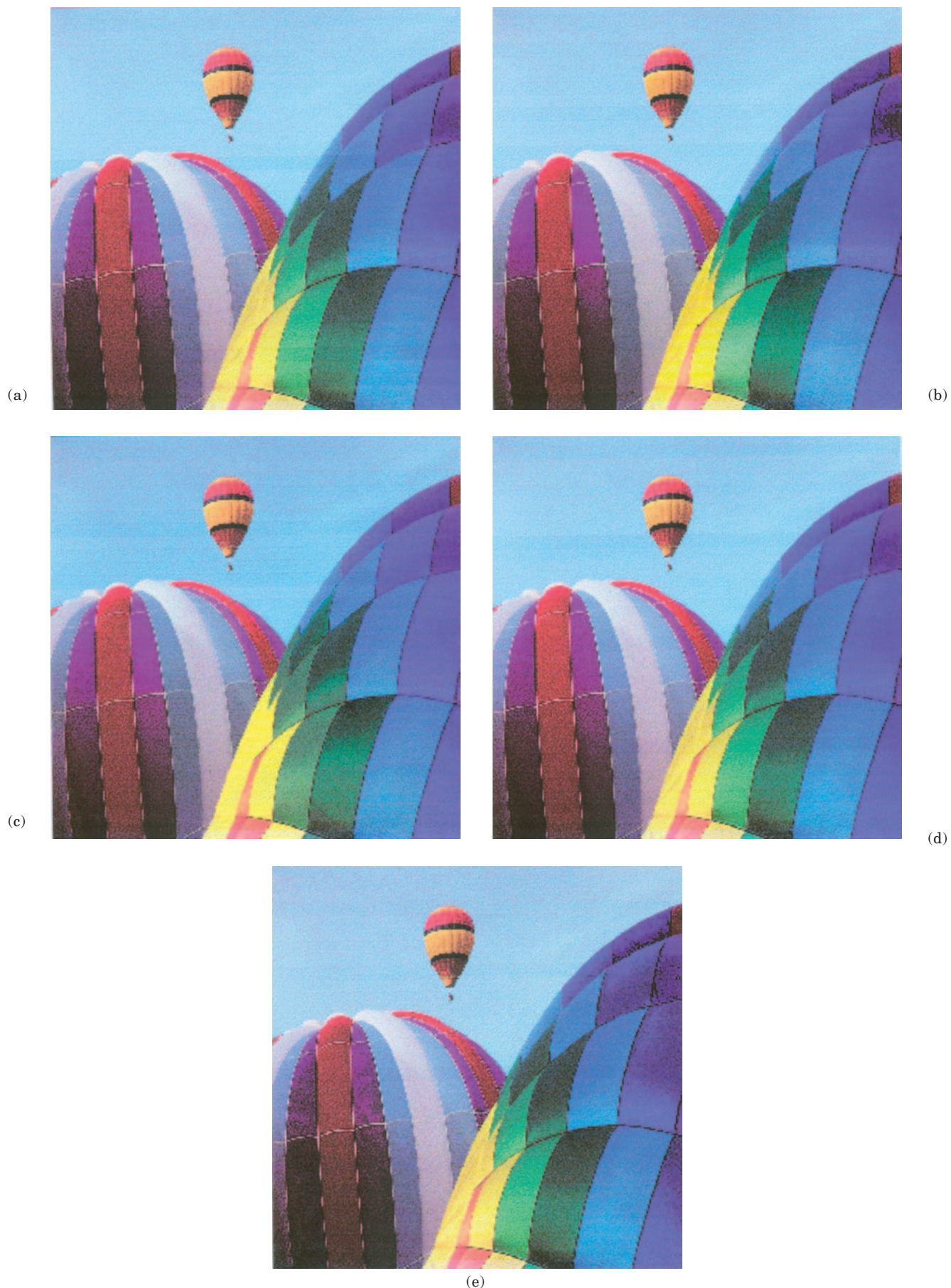


(d)



(e)

Color Plate 5. 'Fresh' image printed by various GMAs; (a) linear lightness compression and clipping chrominance, (b) linear lightness compression and linear chrominance compression, (c) CUSP method, (d) variable anchor point method, (e) proposed method. (Cho, et al., pp. 66–74)



Color Plate 6. 'Balloon' image printed by various GMAs; (a) linear lightness compression and clipping chrominance, (b) linear lightness compression and linear chrominance compression, (c) CUSP method, (d) variable anchor point method, (e) proposed method. (Cho, *et al.*, pp. 66–74)



(a)



(b)



(c)



(d)



(e)

Color Plate 7. 'Parrots' image printed by various GMAs; (a) linear lightness compression and clipping chrominance, (b) linear lightness compression and linear chrominance compression, (c) CUSP method, (d) variable anchor point method, (e) proposed method. (Cho, *et al.*, pp. 66–74)



(a)



(b)



(c)



(d)



(e)

Color Plate 8. ‘Motocycle’ image printed by various GMAs; (a) linear lightness compression and clipping chrominance, (b) linear lightness compression and linear chrominance compression, (c) CUSP method, (d) variable anchor point method, (e) proposed method. (*Cho, et al.*, pp. 66–74)



(a)



(b)



(c)



(d)



(e)

Color Plate 9. 'Boat' image printed by various GMAs; (a) linear lightness compression and clipping chrominance, (b) linear lightness compression and linear chrominance compression, (c) CUSP method, (d) variable anchor point method, (e) proposed method. (Cho, *et al.*, pp. 66–74)